Short Papers

Estimation and Compensation of Subpixel Edge Localization Error

Federico Pedersini, Augusto Sarti, and Stefano Tubaro

Abstract—We propose and analyze a method for improving the performance of subpixel Edge Localization (EL) techniques through compensation of the systematic portion of the localization error. The method is based on the estimation of the EL characteristic through statistical analysis of a test image and is independent of the EL technique in use.

Index Terms—Feature extraction, edge localization, subpixel detection.

———————————— ◆ ————————————

1 INTRODUCTION

A precise localization of image edges can be of critical importance for certain image applications, such as 3D reconstruction, photogrammetry, remote sensing, and automatic inspection [1]. Luminance edges, in fact, are important not only for the fact that they normally carry significant information about the imaged scene [2], [3], but also for the fact that they allow us to extract 3D information on the geometry of the scene which is being imaged.

The accuracy of typical edge detection algorithms [3], [4] is limited by the CCD camera resolution, which can be increased only at very high costs. In alternative, one could look into the possibility of using subpixel feature localization algorithms in order to reach super-resolution performance with low-cost CCD cameras [1], [6].

In order to solve the edge localization (EL) problem with subpixel accuracy, it is necessary to have some a priori information about the nature of both image edges and acquisition systems. In fact, as the CCD camera performs image sampling, its model is not invertible for all signals. In particular, signals having high-frequency components, such as abrupt luminance transitions (edges), cannot be retrieved beyond pixel resolution. In order to overcome the limitation represented by Shannon's sampling theorem, we may look at the subpixel edge localization problem as that of inverting the camera model for a very specific class of signals. This corresponds to determining the parameters of a specified edge transition model that, when cascaded with the camera model, produces the available digital image.

In this article, we propose and evaluate a method for improving the performance of subpixel edge localization techniques, based on the correction of the Edge Localization Error (ELE), which performs at its best on low-noise images, such as camera calibration patterns. The method is particularly useful in those applications where the accuracy of edge localization is more important than noise suppression [16] and acts on nearly-horizontal or nearly-vertical edges, i.e., where the ELE is the heaviest. In Section 2, we describe an accurate model of the acquisition system and, in particular, that of a CCD camera, while a characterization of the ELE is given in Section 3. In Section 4, we propose and describe a method for estimating the EL function and show how to derive an ELE compensation map from it.

- *The authors are with the Dipartimento di Elettronica e Informazione, Politecnico di Milano, Piazza Leonardo da Vinci, 32, 20133 Milano, Italy. E-mail: pedersin@elet.polimi.it.*

Such a method is based on a statistical analysis of appropriate test images, therefore, we do not need any a priori information either on the camera system or on the adopted subpixel EL technique.

Tests have been performed in order to evaluate the impact of the proposed technique on concrete situations. In particular, we have embedded the ELE compensator into a complete camera calibration procedure. The task of estimating intrinsic and extrinsic camera parameters from the analysis of known image targets [8], [9] is comparatively performed with subpixel detectors with and without ELE-compensation. The results of such experiments, reported in Section 5, show that the performance of the calibration procedure improves significantly when ELE compensation is being employed in the localization algorithm.

2 A MODEL FOR THE ACQUISITION SYSTEM

The imaging systems that we consider in this article are standard TV-resolution CCD cameras, either digital or equipped with a frame-grabber (synchronized with the pixel clock). In either case the acquisition system can be modeled as shown in Fig. 1, where a nonlinear stretching of the image plane, followed by a low-pass filter and an ideal sampler processes the image obtained with an ideal lens ("pin-hole"), which performs a simple perspective projection onto the image plane. In fact, there are roughly two types of aberrations that prevent the lens from behaving ideally: those that cause a local shift of image points (distortion), and those that cause blurring (lens *aperture*, CCD-sensor aperture, curvature of field, astigmatism, coma, etc.) [11], [12].
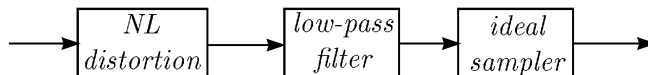

Fig. 1. Overall model of the acquisition system.

Lens distortion causes image points to be shifted from the positions predicted through paraxial approximation. This positional shift mainly occurs along the radial direction from the optical center (intersection between the optical axis and the image plane), in which case it is called *radial distortion* [8]. Radial distortion can be rather accurately described in a compact parametric form by truncating the series expansion $\zeta_u = \zeta_d \left(1 + k_3 \zeta_d^2 + k_5 \zeta_d^4 + \ldots \right)$ that expresses the undistorted radial coordinate ζ_u as a function of the distorted one ζ_d. A truncation of this series to the third-order or fifth-order term is usually sufficient for an accurate description of the positional shift of the image points.

Besides distortion, real lenses always have a low-pass effect on the image, even when the subject is perfectly in focus. As a matter of fact, there always is a bandwidth limitation on the optical lens due to its finite aperture, so that the image $I(x, y)$ that actually forms on the CCD surface is a low-pass version $I(x, y) = h(x, y) * I_g(x, y)$ of the ideal image $I_g(x, y)$, $h(x, y)$ being the impulse intensity response of the lens, whose Fourier transform is known as Modulation Transfer Function (MTF). The MTF is intimately related to the shape of the lens aperture, in fact, it can be obtained by computing, through an appropriate change of variables, the autocorrelation of the *pupil function* (which is equal to one in a circular region that corresponds to the iris diaphragm, and is zero outside this region). The MTF [11] is thus a circularly symmetric low-pass response.

The light coming from the lens focuses on the image plane, i.e., the CCD sensor surface, and forms an analog image, which is sampled over time and space. The sampling process, however, is
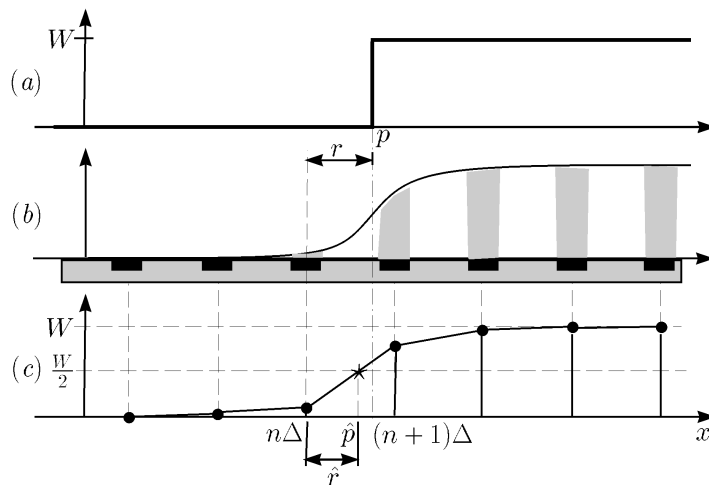
Fig. 2. Subpixel edge detection based on linear interpolation. (a) Ideal luminance profile. (b) Luminance profile incident on the image plane. (c) Linear interpolation of the image samples.

not ideal as the photosensitive regions have a nonnegligible size and the time-integration period is not zero. The total light intensity falling on each photosensitive area, for example, is integrated over a *shutter* period, which is less than or equal to a frame period. As far as spatial sampling is concerned, the light is integrated over the photosensitive area of each pixel. This operation can be modeled by a low-pass filter followed by an ideal 2D spatial sampling over a grid defined by the geometry of the CCD sensor. The spatial impulse response of the cell, which is normally called *CCD aperture function*, corresponds to the light sensitivity map associated to a pixel cell [10], and is normally assumed to be $W_{cell}(x, y) = 1$ inside the photosensitive region and zero outside. The luminance sample $I_{h,k}$ associated to a pixel is thus proportional to the amount of energy absorbed in one shutter period by its photosensitive area $\mathcal{P}_{h,k}$, i.e.,

$$I_{h,k} = \iint_{\mathcal{P}_{h,k}} I(x, y)dx\,dy = \iint I(x, y)W_{cell}\left(x - h\Delta_x, y - k\Delta_y\right)dx\,dy,$$

where pixels are assumed to be organized on a rectangular grid whose horizontal and vertical sampling intervals correspond to their relative intercell distances Δ_x and Δ_y. Notice that the actual size of the photosensitive area is smaller than the size of the pixel cell (usually about one third of the whole cell area [5]).

If the camera is not digital, after the readout process, the analog stream of luminance samples of the CCD array is first processed by a charge amplifier and then by a line amplifier. Image digitization is then performed by a frame grabber through resampling and quantization. The cascade of the *charge* amplifier and the *line* amplifier can be modeled as a low-pass filter whose cut-off frequency is half the pixel clock frequency [14]. As the 1D analog video signal is a time-sequential scanning of the 2D image, filtering the analog 1D signal corresponds to filtering the 2D signal only in the horizontal direction. As a consequence, the bandwidth of CCD images is normally wider along columns than along rows.

As far as other types of aberrations such as curvature of field, astigmatism and coma are concerned, they can either be neglected or included in the low-pass transfer function that models the limited lens and CCD-sensor aperture [11], [12]. In conclusion, the lens (radial/tangential) distortion is all included in the first block of Fig. 1, while all sources of blurring (lens aperture, aberrations, CCD sensor aperture, etc.) are all included in the second block.

Notice that step-like luminance transitions undergoing lens distortion remain step-like, therefore, if our goal is that of recovering the location of the transition with subpixel accuracy, we can compensate for the distortion *after* edge localization. This corresponds to "incorporating" lens distortions into the imaged scene and localizing the edges of a "distorted universe," while leaving the task of unwarping the universe to afterwards. This operation is possible if we have a reliable estimate of the distortion coefficients, which can be obtained through camera calibration [8], [9].

As far as noise is concerned, the most relevant sources in a CCD camera are "dark current" noise, "fat-zero" noise, and "reset" [13], [15]. Such types of noise are well modeled by an additive gaussian noise. Furthermore, the digitization process introduces a certain *quantization error* in the analog-to-digital conversion. This type of noise can be neglected if an adequate number of quantization levels is available.

In general, CCD cameras are designed in such a way to guarantee that the internally generated noise is not greater than quantization noise. If the number of quantization levels is 256, in the worst case of bilinear interpolation and quantization errors of the same sign, the edge trabsition results as vertically shifted of $\Delta/2$, Δ being the quantization step. Such a vertical transition is to be compared with a total edge transition of approximately 60Δ to 80Δ. The impact of such a relative vertical shift on the edge localization is definitely below the tolerance of construction of a standard TV-resolution CCD sensor. In conclusion, both internally generated noise and quantization error can be neglected for the problem approached in this paper.

3 EDGE LOCALIZATION ERROR

The subpixel EL methods that are currently available in the literature are all characterized by different levels of accuracy and noise-rejection. Depending on the strategy adopted by the subpixel method, the ELE associated to it may exhibit a certain *systematic* character [1], [6], [7]. It is quite evident that, if we can completely characterize and predict the ELE, then we can also compensate for it.

Dealing with image edges that are either nearly horizontal or nearly vertical greatly simplifies the analysis and the characterization of the ELE, as the problem becomes one-dimensional. We will see later on, however, that limiting our analysis to the case of nearly horizontal or nearly vertical edges does not represent a serious loss of generality, as the edges that predominantly suffer from a systematic ELE are the horizontal and the vertical ones.

The 1D ELE corresponding to an abrupt luminance transition is the distance between the sharp transition that would form on the image plane when using an *ideal* optical lens and the edge that has been actually detected. It is quite clear that, besides depending on
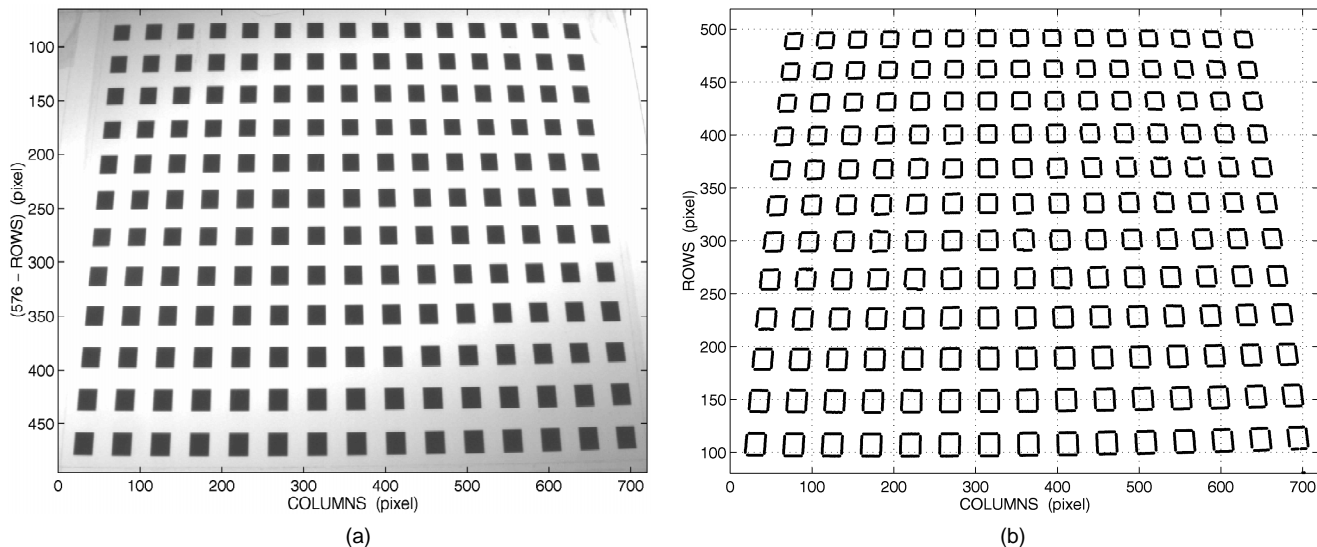
Fig. 3. (a) Test image used for the estimation of the error compensation function and for camera calibration. (b) Edges extracted from the test image.

the acquisition system, the ELE critically depends on the subpixel EL technique under exam. In order to clarify the concept, let us consider the simplified situation shown in Fig. 2, where a sharp luminance transition occurring at the coordinate p on the image axis (horizontal or vertical coordinate of the image plane) is being localized at subpixel precision by using of a simple linear interpolation technique.

The luminance profile of Fig. 2a is a section of what would be imaged on the image plane if an *ideal* lens were used instead of the real one. Due to the limited aperture of the lens, the actual luminance profile is a filtered version of the ideal one, as shown in Fig. 2b. When the light reaches the array of photosensors of the CCD camera, the image is spatially sampled. The luminance samples that are actually collected by the CCD array, however, are not the result of an ideal sampling of the luminance profile of Fig. 2b, as they depend on the light that falls on the whole photosensitive area of the pixel. In fact, assuming that the photosensitive area is equally sensitive to the light, each luminance sample is given by the area of the shaded regions in Fig. 2b, as shown in Fig. 2c.

A simple way of estimating the subpixel location p of the ideal edge from the samples collected from the CCD array consists of linearly interpolating (see Fig. 2c) the collected samples, and determining the intersection between the resulting piecewise linear profile and an appropriate threshold. The threshold is set equal to half the amplitude W of the luminance discontinuity, and the resulting intersection can be taken as an estimate of the edge location. Such an example of subpixel EL method is simple enough to visualize the ELE associated to it, in fact the estimated edge location $\hat{p}$ differs from the ideal location p of a quantity called Edge Localization Error e. It is not difficult to realize that the ELE is a periodic function of the edge location, provided that some conditions of regularity in the acquisition system are satisfied (basically a homogeneous CCD array). In this case, it is convenient to refer ideal and estimated edge locations to the center of the pixel immediately before the ideal edge location and limit the description to one period of it.

In what follows, the function that maps the ideal relative edge location r into the estimated one $\hat{r}$ is called Edge Localization Function (ELF), $\hat{r} = F_{EL}(r)$, and the ELE can be written in terms of the ELF as follows

$$e = \hat{r} - r = E_{ELE}(r) = F_{EL}(r) - r \qquad (1)$$

4 ERROR COMPENSATION

As already mentioned in Section 3, if the ELF $\hat{r} = F_{EL}(r)$ is an invertible function of the local coordinate r of the 1D (horizontal or vertical) image axis, then we can compensate for the ELE provided that a reliable ELF is available. In this section, we show how to estimate the ELF and how to derive the relative compensation function through statistical analysis of some test images.

4.1 Estimation of the Error Characteristic

With reference to Fig. 2, we have seen in Section 3 that the estimated (affected by ELE) relative edge location $\hat{r}$ can be seen as a function $F_{EL}(r)$ (*EL function*) of the actual (ideal) relative edge location r. Since the response of the CCD camera can be considered space-invariant, the *ELE* function $e = \hat{r} - r = E_{EL}(r)$, must be periodic of period 1 pixel, therefore, we can limit our analysis, for example, to any interval like $r_0 \le r \le 1 + r_0$. The periodicity of the ELE and (1) results in $1 + \hat{r} = F_{EL}(1 + r)$. If $F_{EL}(r)$ is monotonic, then it is also bijective, in which case its inverse function, $r = F_{EL}^{-1}(\hat{r})$ is bijective as well. The output range corresponding to $r_0 \le r \le 1 + r_0$ results as $\hat{r}_0 \le \hat{r} \le 1 + \hat{r}_0$, where $\hat{r}_0 = F_{EL}(r_0)$. The inverse $F_{EL}^{-1}(\cdot)$ of the ELF can thus be used as an *error compensation function*.

As the ELF is a map from the ideal edge locations onto the detected edge locations, we can derive information on it from the joint statistics of both its input and its output. The estimation of the error compensation function, in fact, can be done through statistical analysis of an appropriate test image. The statistical distribution of the estimated edge locations can be quite easily extracted from the test image, while the statistics of the ideal edge location can be inferred from the pattern characteristics in particular cases. From a practical viewpoint, it is convenient to choose test images whose ideal edge points (referred to the center of the pixel area that they fall on) are uniformly distributed over pixel areas. An example of image that satisfies these requirements is reported in the next section (see Fig. 3a).

In order to avoid confusion in the notation, in what follows we will denote with capital letters (R and $\hat{R}$) the random variables that represent ideal and estimated fractional edge locations, while
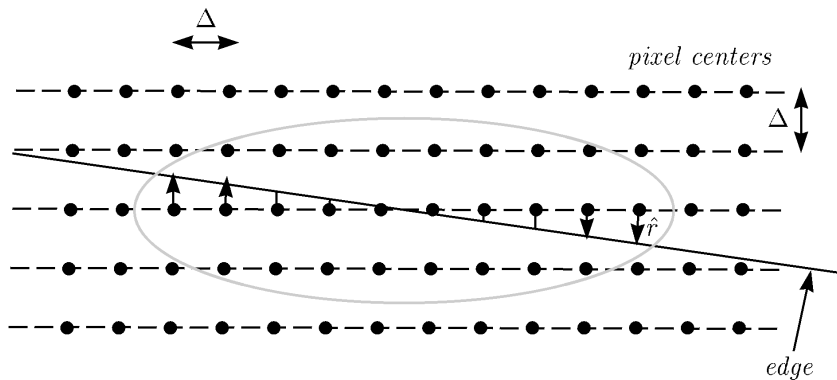
Fig. 4. Construction of the histogram of the local edge coordinates.

lowercase letters (r and $\hat{r}$) will be used for denoting the corresponding instances.

If the probability density function (p.d.f.) of the ideal edge point position R is uniform

$$f_R(r) = \begin{cases} 1 & \text{for } r_0 \leq r < 1 + r_0 \\ 0 & \text{elsewhere} \end{cases} \tag{2}$$

then the p.d.f. of $\hat{R} = F_{EL}(R)$ can be expressed as

$$F_{\hat{R}}(\hat{r}) = \frac{f_R(r)}{F'_{EL}(r)}, \quad r = F_{EL}^{-1}(\hat{r}), \tag{3}$$

where $\hat{r}_0 \leq \hat{r} < 1 + \hat{r}_0$, $F'_{EL}(r)$ is the first derivative of $F_{EL}(r)$, and the absolute value can be omitted in the denominator of (3) as $F_{EL}(r)$ is assumed to be a monotonically increasing function. By replacing (2) into (3) and by applying a property of derivatives, we obtain

$$F_{\hat{R}}(\hat{r}) = \frac{1}{F'_{EL}(r)}\bigg|_{r=F_{EL}^{-1}(\hat{r})} = \frac{d}{d\hat{r}} F_{EL}^{-1}(\hat{r}), \tag{4}$$

where $r_0 \leq r < 1 + r_0$ and $\hat{r}_0 \leq \hat{r} < 1 + \hat{r}_0$.

By integrating the p.d.f. of the subpixel edge locations $\hat{R}$ detected from the image we obtain the compensation function

$$r = C(\hat{r}) = F_{EL}^{-1}(\hat{r}) = F_{EL}^{-1}(\hat{r}_0) + \int_{\hat{r}_0}^{\hat{r}} f_{\hat{R}}(a)\, da. \tag{5}$$

Notice that the value of $\hat{r}_0$ is not a known parameter, therefore, all that we can obtain from the analysis of the image is the statistical distribution of $\hat{R}$, computed over an arbitrary pixel-wide interval like $(A, 1 + A)$, generally not entirely contained in the interval $(\hat{r}_0, 1 + \hat{r}_0)$. Equation (5) could thus be expressed as follows:

$$r = \int_{\hat{r}_0}^{A} f_{\hat{R}}(a)\, da + \int_{A}^{\hat{r}} f_{\hat{R}}(a)\, da + r_0 = \int_{A}^{\hat{r}} f_{\hat{R}}(a)\, da + K_A. \tag{6}$$

It is quite clear from (6) that different choices of the interval of definition of $\hat{r}$ result in different vertical offsets K_A for the compensation function.

Notice that (5) can be used to compute $F_{EL}^{-1}(\hat{r})$ only for $A \leq \hat{r} \leq 1 + A$. Since $E_{EL}(r)$ is a periodic function of period 1 pixel, we extend the range of $F_{EL}(\cdot)$ and $F_{EL}^{-1}(\cdot)$ by using the relationships

$$\begin{aligned} F_{EL}(r + k) &= k + F_{EL}(r) \\ F_{EL}^{-1}(\hat{r} + k) &= k + F_{EL}^{-1}(\hat{r}) \end{aligned} \quad k = 0, \pm 1, \pm 2, \ldots. \tag{7}$$

therefore, if $A \leq \hat{r} \leq A + 1$, then we can use (5), otherwise we can always find an integer k such that $\hat{r} = \hat{r}' + k$, $A \leq \hat{r}' \leq A + 1$, and use (7).

It is worth emphasizing that the fact that the compensation function is derived from a p.d.f. through integration gives us no information on the offset K_A, which means that we can linearize the ELF (i.e., eliminate its ripple), but we still need to determine its offset. The extra unknown can be determined by using further a priori information on the test image, or through camera calibration.

4.2 The Estimation Procedure

The test image of Fig. 3 exhibits edges that are oriented in the vertical and horizontal directions. We will see in the next section that this image is the same one that we use for camera calibration. Notice that the fact that the luminance edges are slightly tilted guarantees their detected subpixel location to have uniform statistical distribution, as required. Notice also that the presence of barrel distortion does not affect the accuracy of the estimation of the ELE characteristic. In fact, the edge coordinates can be assumed as being uniformly distributed over pixel areas when the edges can be considered as *locally* straight in the absence of ELE, which is true also in the presence of barrel distortion.

All edge points of the test image are localized with subpixel accuracy by using an edge localization algorithm, for example one based on cubic interpolation (with the edge location given by the flex point), or even one based simply on linear interpolation. From each edge coordinate x, we compute the local edge coordinate $\hat{r} = \hat{x} - n\Delta$, where the pixel center $n\Delta$ is the nearest one to $\hat{x}$. Assuming that the above lengths are measured in pixels, we have $-\frac{1}{2} \leq e \leq \frac{1}{2}$ and $A = -\frac{1}{2}$. The p.d.f. $f_{\hat{R}}(\hat{r})$ of the detected subpixel relative locations is estimated by building a histogram for $\hat{r}$, as shown in Fig. 4. This operation corresponds to building a piecewise constant approximation of the desired p.d.f., and then normalizing its amplitude. Finally, we integrate $f_{\hat{R}}(\hat{r})$ in order to compute the first term of (6). As far as the offset K_A is concerned, as we will see in Section 5, its determination depends on the specific application.

Fig. 5a shows an example of the p.d.f. $f_{\hat{F}}(b)$ that is estimated from the test image (only the edges localized along columns). Compensation is performed by using (6) and the resulting *compensation function* $C(\hat{r}) = F_{EL}^{-1}(\hat{r})$, is shown in Fig. 5b. The compensated edge position r is then obtained by simply applying the compensation $C(\hat{r})$ to the detected position $\hat{r}$, i.e., $r = F_{EL}^{-1}(\hat{r}) = C(\hat{r})$.

Notice that the compensation method described above does not depend on the choice of subpixel edge localization technique that is being used. However, it is reasonable to expect cubic interpolation to outperform linear interpolation in the edge placement because of a different noise rejection. In fact, a cubic interpolator averages over a larger number of samples, thus reducing the noise.

5 AN EXAMPLE OF APPLICATION

In order to improve the performance of an EL technique through the ELE compensation method of Section 4 we first need to perform subpixel edge localization on the *test* image and then estimate the
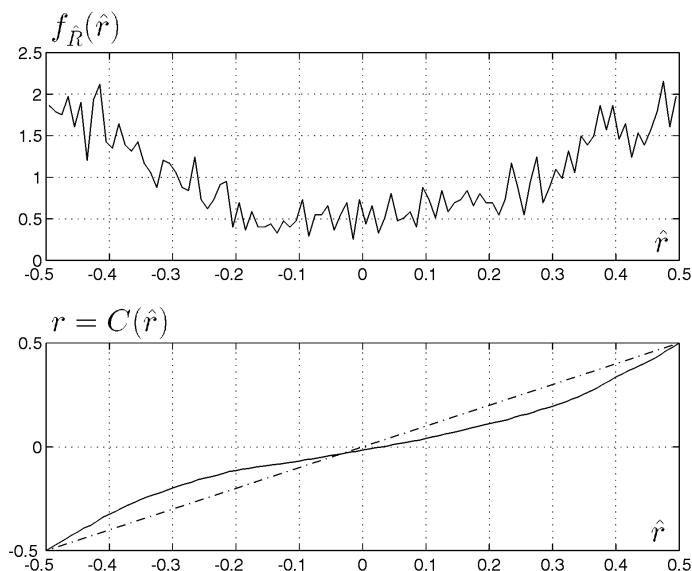
Fig. 5. (a) Estimated p.d.f. of the detected subpixel residuals. (b) Relative compensation function.

compensation curve from the extracted edge points. At this point we can perform subpixel edge localization on the *scene* image and correct the edge coordinates through the estimated compensation function. Notice that, if the edge points in the scene image satisfy condition (2), then the ELE results as being uniformly distributed, therefore the scene image can be used also as a test image.

In order to evaluate the impact of the above compensation technique on the performance of a subpixel edge localizator, we have embedded the method into a camera calibration procedure [8], [9] and compared the results with and without compensation. Camera calibration consists in estimating *intrinsic* and *extrinsic* parameters of an image acquisition system through the analysis of the views of a *calibration pattern*. In the adopted camera model, the intrinsic parameters are the *optical center* (intersection between the optical axis and the image plane), the *focal length* and two parameters that describe the radial nonlinear distortion of the optical lens. The extrinsic parameters are represented by the relative position and orientation of the camera with respect to the target. It is quite evident that the reliability of the calibration procedure critically depends on how accurately certain *fiducial marks* of the calibration pattern are localized.

As already said in the previous section, the calibration pattern used in the experiment is the same test image that we used for the estimation of the ELE's statistics. Such a target is planar and exhibits a set of regularly spaced black squares on a white background, as shown in Fig. 3. The position of the fiducial marks on the target, i.e., the corner points of the squares, is known with a precision of ± 5μm. In order to perform an accurate camera calibration, it is necessary to localize the fiducial marks of the test image with the best achievable precision. Being the fiducial marks corner points of squares, they can be localized by intersecting edges detected with subpixel accuracy.

The adopted calibration procedure estimates the camera parameters and provides us with a measure of the estimate's accuracy, based on the standard deviation of the error between the detected position of fiducial marks on the image plane, and their position computed through the camera model. The accuracy measurement has been used as an evaluation of the performance of the edge localization algorithm, and a comparative evaluation of the results with and without ELE compensation has been done. As already mentioned in Section 4, the ELE compensation requires the determination of offset parameters. In fact, the offsets have

been added to the list of intrinsic parameters of the CCD camera and estimated by the calibration procedure. By doing so, the estimated offsets can be used in other applications and for the ELE correction.

The ELE statistics associated to the test image of Fig. 3 can be assumed uniform with good approximation, therefore the calibration target is suitable also for the estimation of the compensation curve. The edge points of the test image are obtained with a technique based on cubic interpolation and flex point search. From such edges it is quite straightforward to visualize the ELE associated to the adopted subpixel technique. In fact, by magnifying all horizontal (vertical) edges of one row (column) of squares, we obtain the curves of Fig. 6, whose oscillations are mainly caused by the ELE. By comparing the curves of Fig. 6, obtained with and without compensation, we observe a substantial reduction of the ELE.

In order to quantify the impact of the compensation method on the accuracy of the calibration, we measured the standard deviation of the calibration points before and after its adoption. The standard deviation dropped from 0.081 pixel to 0.045 pixel, which corresponds to an improvement of about 44 percent.

Notice that the proposed ELE compensation method is one-dimensional, as it can be applied to either nearly horizontal or nearly vertical edges. Extensions to the more general two-dimensional case are possible by taking into account the fact that we would have to construct an approximation of two EL surfaces (two EL functions of two parameters). In fact, we would need to express position and orientation of a detected edge as a function of position and orientation of the ideal edge that generated it. It is worth noticing, however, that edges that are either nearly horizontal or nearly vertical are the most sensitive to ELE. In fact, with reference to Fig. 6, it is not difficult to realize that the density of ripples due to ELE increases with the edge angle with respect to horizontality or verticality. In particular, a nearly-horizontal edge gives rise to a very *slow* ripple. In this case, we can correctly estimate the actual edge location only when a large number of edge points is available. ELE compensation allows us to dramatically reduce such a number. As the edge slope increases, the ripple periodicity increases as well, which makes ELE compensation progressively less useful.
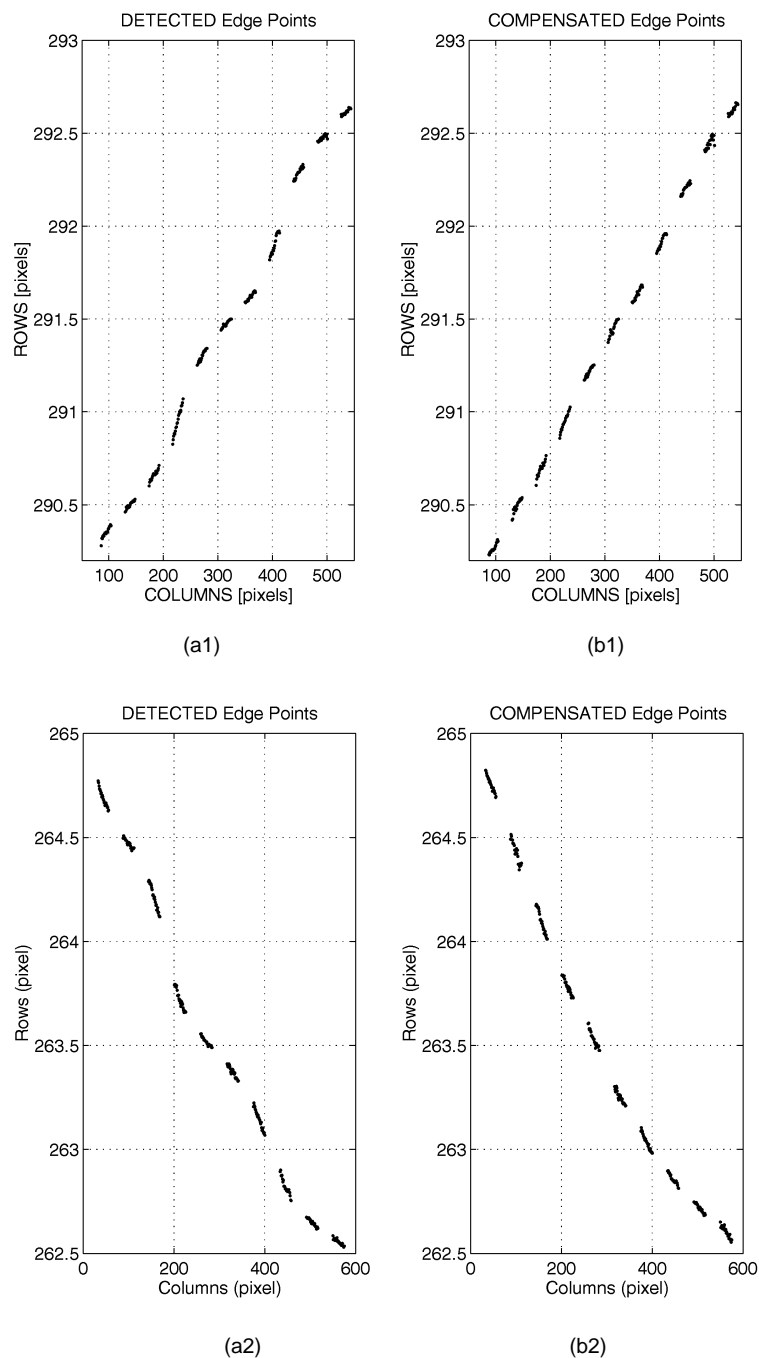
Fig. 6. (a1, b1) Magnification of rows 290-293. (a2, b2) Magnification of rows 262-265 of Fig. 3b. (a) Linear interpolation and threshold crossing. (b) Same as (a) with error compensation.

6 CONCLUSIONS

In this article, we have proposed and analyzed a method for improving the performance of subpixel edge localization techniques, which is based on the compensation of their ELE. In particular, we have shown how to estimate the EL function and how to derive the ELE compensator from it. We have also evaluated the performance of the ELE compensation method in a concrete situation, by determining its impact on the accuracy of a camera calibration procedure.

The improvement in the calibration accuracy due to ELE compensation has been shown to be quite significant (44 percent), which can be crucial especially in applications of low-cost photo-grammetry and 3D reconstruction from multiple views, and justifies its adoption whenever it is important to maximize the precision of the edge localization without significantly affecting the total cost of the acquisition system.

REFERENCES

[1] G.A.W. West and T.A. Clarke, "A Survey and Examination of Subpixel Measurement Techniques," *Proc. SPIE, vol. 1,395, "Close-Range Photogrammetry Meets Machine Vision,"* pp. 456-463, 1990.

[2] D.C. Marr and T. Poggio, "A Theory of Human Stereo Vision," *Proc. Royal Soc. London*, vol. B 204, pp. 301-328, 1979.

[3] J. Canny, "A Computational Approach to Edge Detection," *IEEE Trans. Pattern Analysis and Machine Intelligence*, vol. 8, no. 6, Nov. 1986.

[4] R. Deriche, "Fast Algorithms for Low-Level Vision," *IEEE Trans. Pattern Analysis and Machine Intelligence*, vol. 12, no. 1, Jan. 1990.

[5] R. Lenz and U. Lenz, "New Developments in High Resolution Image Acquisition With CCD Area Sensors," *Optical 3D Measurement Techniques II*, Zurich, Switzerland, Oct. 1993, Wichmann.

[6] R.J. Walkenburg, A.M. McIvor, and P.W. Power, "An Evaluation of Subpixel Feature Localisation Methods for Precision Measurement," *Proc. SPIE, Videometrics III*, vol. 2,350, pp. 229-238, 1994.

[7] I. Maalen-Johansen, "On the Precision of Subpixel Measurements in Videometry," *Proc. ISPRS '93*, Zurich, Switzerland, Oct. 1993.

[8] R. Tsai, "A Versatile Camera Calibration Technique for High-Accuracy 3D Machine Vision Metrology Using Off-the-Shelf TV Cameras and Lenses," *IEEE J. Robotics and Automation*, vol. 3, no. 4, pp. 323-344, Aug. 1987.

[9] F. Pedersini, S. Tubaro, and F. Rocca, "Camera Calibration and Error Analysis: An Application to Binocular and Trinocular Stereoscopic Systems," *Fourth Int'l Workshop Time-Varying Image Processing and Moving Object Recognition*, Florence, Italy, June 1993.

[10] S.G. Chamberlain and D.H. Harper, "MTF Simulation Including Transmittance Effects and Experimental Results of Charge-Coupled Imagers," *IEEE Trans. Electron Devices*, vol. 25, no. 2, Feb. 1978.

[11] J.W. Goodman, *Introduction to Fourier Optics*. McGraw-Hill, 1968.

[12] M. Born and E. Wolf, *Principles of Optics*. Pergamon Press, 1959.

[13] D.F. Barbe, "Imaging Devices Using the Charge-Coupled Concept," *Proc. IEEE*, vol. 63, no. 1, Jan. 1975.

[14] J. Hynecek, "Design and Performance of a High-Resolution Image Sensor for Color TV Applications," *IEEE Trans. Electron Devices*, vol. 32, no. 8, Aug. 1985.

[15] J. Hynecek, "Spectral Analysis of Reset Noise Observed in CCD Charge-Detection Circuits," *IEEE Trans. Electron Devices*, vol. 37, no. 3, Mar. 1990.

[16] R. Mehrotra and S. Zhan, "A Computational Approach to Zero-Crossing-Based Two-Dimensional Edge Detection," *Graphical Models and Image Processing*, vol. 58, no. 1, pp. 1-17, Jan. 1996.